

Wiejak, J., Tsimbouri, P.M., Herzyk, P., Dalby, M.J., Hamilton, G., and Yarwood, S.J. (2013) Genomic analysis of the role of transcription factor C/EBP δ in the regulation of cell behaviour on nanometric grooves. *Biomaterials*, 34 (8). pp. 1967-1979. ISSN 0142-9612

Copyright © 2012 Elsevier Ltd.

A copy can be downloaded for personal non-commercial research or study, without prior permission or charge

The content must not be changed in any way or reproduced in any format or medium without the formal permission of the copyright holder(s)

When referring to this work, full bibliographic details must be given

<http://eprints.gla.ac.uk/73803>

Deposited on: 09 January 2013



Genomic analysis of the role of transcription factor C/EBP δ in the regulation of cell behaviour on nanometric grooves

Jolanta Wiejak¹, Penelope M. Tsimbouri¹, Pawel Herzyk, Matthew J. Dalby, Graham Hamilton, Stephen J. Yarwood*

Institute of Molecular, Cell and Systems Biology, College of Medical, Veterinary and Life Sciences, University of Glasgow, Glasgow, United Kingdom

ARTICLE INFO

Article history:

Received 1 November 2012

Accepted 20 November 2012

Available online 13 December 2012

Keywords:

Nanotopography

Cell signalling

Cell spreading

Cell adhesion

Gene expression

Signal transduction mediator

ABSTRACT

C/EBP δ is a tumour suppressor transcription factor that induces gene expression involved in suppressing cell migration. Here we investigate whether C/EBP δ -dependent gene expression also affects cell responses to nanometric topology. We found that ablation of the C/EBP δ gene in mouse embryonal fibroblasts (MEFs) decreased cell size, adhesion and cytoskeleton spreading on 240 nm and 540 nm nanometric grooves. ChIP-SEQ and cDNA microarray analyses demonstrated that many binding sites for C/EBP δ , and the closely related C/EBP β , exist throughout the mouse genome and control the upregulation or downregulation of many adjacent genes. We also identified a group of C/EBP δ -dependent, *trans*-regulated genes, whose promoters contained no C/EBP binding sites and yet their activity was regulated in a C/EBP δ -dependent manner. These genes include signalling molecules (e.g. SOCS3), cytoskeletal components (Tubb2, Krt16 and Krt20) and cytoskeletal regulators (ArhGEF33 and Rnd3) and are possibly regulated by *cis*-regulated diffusible mediators, such as IL6. Of particular note, SOCS3 was shown to be absolutely required for efficient cell spreading and contact guidance on 240 nm and 540 nm nanometric grooves. C/EBP δ is therefore involved in the complex regulation of multiple genes, including cytoskeletal components and signalling mediators, which influence the nature of cell interactions with nanometric topology.

© 2012 Elsevier Ltd. All rights reserved.

1. Introduction

C/EBP proteins form a highly conserved family of leucine zipper (bZIP) transcriptional factors that serve as master regulators of cellular processes such as the cell cycle, differentiation, and inflammatory responses [1]. So far, six C/EBP genes have been isolated (α , β , γ , δ , ϵ , and ζ), although protein numbers may well be higher due to variation in polypeptide size through alternate splicing and protein processing [2]. C/EBP isoforms are structurally similar, displaying a characteristic basic leucine zipper domain at the C terminus (90% homology between isoforms), which facilitates dimerization and DNA binding [2]. However, C/EBP isoforms are functionally and genetically distinct, with their transcriptional

activation domains less well conserved (<20% sequence identity between isoforms). This divergence gives rise to the wide range of cellular responses in which C/EBP isoforms have been implicated [2].

Attention has recently turned to the functional role of the C/EBP δ isoform, which represents a ubiquitously expressed transcriptional activator that is robustly induced in a variety of G₀ growth arrested cells [3]. Importantly, “loss of function” alterations in C/EBP δ have been reported in breast cancer [4–6] and acute myeloid leukaemia (AML) [7] and are generally associated with impaired contact inhibition, increased genomic instability and increased cell migration [8]. The use of knockout mice demonstrated that C/EBP δ has a vital role in mammary duct and epithelial cell proliferation [9] as well as an obligate role in the differentiation of preadipocytes [10,11]. In addition, recent work suggests that C/EBP δ is required for the maintenance of pluripotency in human limbic stem cells [2]. C/EBP δ activity appears to be regulated at a number of levels, including transcriptional (gene induction by STAT3, Sp1, CREB and NcoA/SRC-1 [12,13]), post-transcriptional (mRNA stability [14]) and post-translational (ubiquitinylation [15] and SUMOylation [16]) mechanisms. Certain C/EBP isoforms have also been shown to be substrates for various protein kinases, including the MAP kinases,

* Corresponding author. Institute for Molecular, Cell and Systems Biology, College of Medical, Veterinary and Life Sciences, University of Glasgow, Room 239, Davidson Building, Glasgow, Scotland G12 8QQ, United Kingdom. Tel.: +44 (0)141 330 3908; fax: +44 (0)141 330 4620.

E-mail addresses: S.Yarwood@bio.gla.ac.uk, stephen.yarwood@glasgow.ac.uk (S.J. Yarwood).

¹ These authors contributed equally to research.

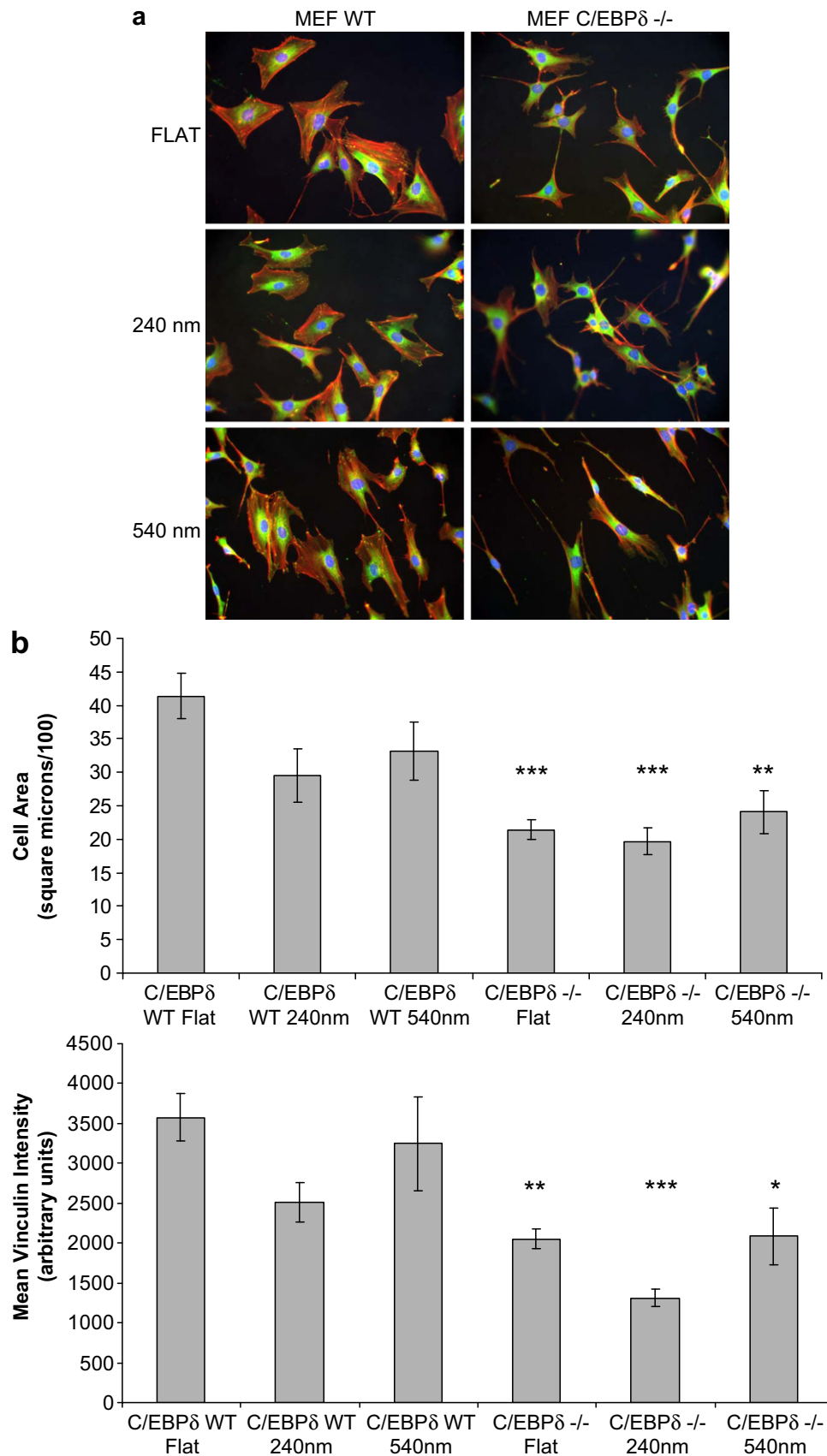


Fig. 1. Morphology of wild type (WT) and C/EBP δ $-/-$ mouse embryonic fibroblasts (MEFs) cultured on flat or nanogrooved substrates. a) MEF WT and MEF C/EBP δ $-/-$ cells were cultured on flat or nanogrooved substrates as indicated and stained for actin cytoskeleton (red) and vinculin (green). MEF WT cells had a well developed actin cytoskeleton and a largely polygonal morphology and became bipolar when cultured on grooves. In contrast C/EBP δ $-/-$ MEFs had a less well developed actin cytoskeleton, were generally smaller and became very elongated when grown on the grooved substrate. b) MEF WT and MEF C/EBP δ $-/-$ cell area and vinculin intensity were quantified as described in *Materials and Methods*. Results demonstrated that MEF C/EBP δ $-/-$ cells were smaller and had lower levels of vinculin, on both flat and grooved surfaces, than MEF WT cells. (For interpretation of the references to colour in this figure legend, the reader is referred to the web version of this article.)

ERK 1 and 2, and protein kinase C (PKC) [1], and are targets of second messenger signalling pathways. For example, elevations in the intracellular levels of cyclic AMP and activation of protein kinase A, has a direct impact on the induction of the constitutively active C/EBP δ isoform, which, in turn, regulates the acute-phase plasma protein gene haptoglobin, which is involved in the intestinal epithelial cell response to inflammation [12], whereas cyclic AMP-activation of exchange protein activated by cyclic AMP 1 (EPAC1), leads to the C/EBP δ -dependent induction of the anti-inflammatory suppressor of cytokine signalling 3 (SOCS3) gene in vascular endothelial cells [17].

Despite being a transcriptional activator, very few C/EBP δ target genes have been identified. As a result the mechanisms by which C/EBP δ controls cell adhesion, migration, differentiation and cell-cycle progression remain poorly understood. Recent reports have demonstrated that sumoylation of C/EBP δ promotes sequestration to the nuclear periphery, thereby suppressing expression of C/EBP δ -dependent genes associated with cell adhesion, including glycoprotein V, protocadherin 9 and integrin β 8 [8,16]. Given this potential link between transcriptional control and cell adhesion we have used genomic analysis (including gene array and high resolution DNA sequencing) to investigate the role of C/EBP δ in controlling cell adhesion with biomaterials, comparing planar and nanometric grooved growth surfaces.

2. Materials and methods

2.1. Materials

Wild type (WT) immortalized mouse embryonic fibroblasts (129SV:C57Cl/6, MEFs) and MEFs containing homozygous deletions of the C/EBP β , or C/EBP δ genes were generous gifts from Prof. Peter Johnson (C/EBP β) and Esta Sterneck (C/EBP δ) from NCI, National Institutes of Health, Frederick, MD. SOCS3 and FAK knockout MEFs, together with matched WT cells, were gifts from Prof. Margaret Frame, Edinburgh Cancer Research UK Centre, UK and Dr Timothy Palmer, Institute of Cardiovascular and Medical Sciences, University of Glasgow, UK, respectively. Forskolin, and rolipram were purchased from Merck Biosciences (Nottingham, UK). Anti-SOCS3 and ChIP-grade, anti-C/EBP polyclonal antibodies were from Santa Cruz.

2.2. Generation of grooved and planar growth surfaces

Microstructured quartz substrates were fabricated by acid-cleaning (7:1H₂SO₄:H₂O₂ for 5 min) quartz slides which were then spin-coated with AZ primer (4000 rpm for 30sec). A layer of Shipley S1818 photoresist (Shipley) was spun onto the spin-coated slides and then soft-baked for 30 min in a 90°C oven. The substrates were UV treated on an MA6 mask aligner with exposure energy of ca. 7.1 mJ/cm² per second in hard contact, through an electron-beam fabricated chrome mask with 12.5 μ m wide lines. The resist was developed (1:1 AZ developer (Microchemicals):water) for 65sec. The substrates were rinsed, dried and then etched in a trichloromethane environment at a rate of 25 nm/min in a reactive ion etching unit (RIE80, Plasma Technology) using the polymer pattern as an etch resist to generate 240 or 540 nm deep grooves. The residual resist was removed with acetone and the slide was blanket etched for a further 1 min to produce a homogenous surface chemistry. Planar slides were blanket etched to ensure that the chemistry was comparable with the structured substrates. Quartz substrates were then cleaned in Caro's acid solution (2:1 H₂SO₄:H₂O₂) for 20 min, rinsed six times with double-distilled water and air-dried under a Class I or II sterile flow hood. Imprints of the quartz substrates into polycaprolactone (PCL) were achieved by hot-embossing. The resulting imprints, 240 nm and 540 nm grooves, were trimmed for use and planar PCL (Ra of 1.17 nm over 10 μ m) was used as a control substrate. The PCL samples were given a 30 s treatment in oxygen plasma to allow cell attachment (Harrick Plasma, USA). All PCL substrates were sterilised in ethanol for 30 min, then transferred through three rinses in sterile 1 \times PBS and two rinses in complete medium.

2.3. Cell culture and growth of cells on biomaterials

Matched wild type (WT) or homozygous knockout (–/–) mouse embryonic fibroblasts (MEFs), for C/EBP β , C/EBP δ , SOCS3 or FAK, were maintained in 71% (v/v) DMEM (Sigma), supplemented with 17.7% (v/v) medium 199, 9% (v/v) FBS, 1% (v/v) 200 mM L-glutamine (Gibco), 0.9% (v/v) 100 mM sodium pyruvate and antibiotics (6.74 U/ml Penicillin-Streptomycin, 0.2 μ g/ml Fungizone) at 37 °C in a 5% CO₂ environment. Cells were passaged at 70–80% confluence, and the medium was replaced regularly. Unless otherwise indicated, MEFs were seeded at a density of 1 \times 10⁴ cells/ml on the PCL thumb-embossed substrates with a 24 h culture period.

2.4. Immunofluorescence

MEFs were fixed in a 10% (v/v) formaldehyde solution (15min at 37 °C), permeabilised (5min at 4 °C) and blocked in 1% (w/v) BSA/PBS (15min at 37 °C). The samples were then stained at 37°C for 1 h with 1:200 (v/v) anti-vinculin (clone hVin-1, Sigma) in 1% (w/v) BSA/PBS and 1:500 (v/v) phalloidin-rhodamine (Molecular Probes). In each experiment, two replicas each of planar and nanogroove topography were stained. Cells were washed 3 \times 5min in 1xPBS containing 0.5% (v/v) Tween-20, and appropriate biotinylated secondary antibody (Vector Laboratories) was added at 1:50 in 1% (w/v) BSA/PBS and incubated for a further hour at 37 °C. After washing, 1:50 (v/v) FITC-conjugated streptavidin (Vector Laboratories) was added to the samples and incubated for 30 min at 4 °C followed by washing and mounting using Vectashield mountant with DAPI nuclear stain (Vector Laboratories). Cell images were captured on a confocal microscope and analysed using Image J software (NIH). Significant changes were determined by one-way ANOVA with Tukey post-test.

2.5. Microarray analysis

C/EBP β WT, C/EBP β –/–, C/EBP δ WT and C/EBP δ –/– cells were grown on planar growth surfaces and then incubated in the presence or absence of a combination of 10 μ M forskolin plus 10 μ M rolipram (F/R) for 5 h at 37 °C in 5% (v/v) CO₂. Cells were then washed with 1 \times 1 ml PBS and RNA was isolated using the Qiagen "RNeasy" Mini Kit according to the manufacturers protocol. RNA samples were additionally treated with a "DNA-free Kit" (Applied Biosystems) to remove any remaining DNA. RNA samples were then prepared for Affymetrix whole transcriptome microarray analysis, using the WT Expression Kit (Ambion) according to the manufacturer's instructions. Briefly, reverse transcription was used to prime poly(A) and non-poly(A), but not ribosomal, mRNA and generate sense strand cDNA for fragmentation and labelling, using the Affymetrix GeneChip® WT Terminal Labelling Kit (PN 900671). Amplified and biotinylated sense-strand DNA targets were hybridised, using a Fluidic Station 400, to Affymetrix GeneChip® Mouse Gene 2.0 ST Array and data captured using an Affymetrix GeneChip® Scanner 3000 7G. Gene expression changes were selected where at least one fold change was greater than 2. Grouping of gene expression data into similarly responsive patterns was done using Treeview and CLUSTER software [18], freely available from the Eisen lab (<http://www.eisenlab.org/eisen/>).

2.6. Chromatin immunoprecipitation and sequencing (ChIP-SEQ) analysis

C/EBP β WT and C/EBP δ WT cells were stimulated in the presence or absence of a combination of 10 μ M forskolin plus 10 μ M rolipram (F/R) for 5 h at 37 °C in 5% (v/v) CO₂. Cells were then fixed and chromatin extracted and sheared using the enzymatic "CHIP-IT Express Kit" (Active Motif) according to the manufacturer's instructions. Sheared chromatin from F/R-treated and non-treated cells was then immunoprecipitated at 4 °C, overnight with 4 μ g of either C/EBP β WT or C/EBP δ ChIP-grade antibodies (Santa Cruz). DNA fragments were eluted from immunoprecipitated chromatin and used to prepare a ChIP-SEQ DNA library for sequencing using the "ChIP-SEQ Sample Prep Kit" from Illumina, according to the manufacturer's protocols. Briefly, the first step in library preparation was to convert any overhangs in the ChIP'd DNA into phosphorylated blunt ends. The 3' ends were then adenylated and adaptors ligated onto the ends of the fragments. The library was then size selected on an agarose gel and eventually enriched by PCR. The enriched library samples were then loaded onto a flow cell at a concentration of 12pM and cluster formation was done on an Illumina Cluster station. Samples were then sequenced on an Illumina GA IIX giving 76bp reads.



2.7. ChIP-SEQ data analysis

The ChIP DNA was sequenced on an Illumina GA IIX, one lane of the flow cell per sample. The quality of the reads was assessed using Fastqc (www.bioinformatics.babraham.ac.uk/projects/fastqc/). The sequence reads were aligned to the mouse genome (release version mm9) using the bowtie aligner (version 0.12.7) (bowtie-bio.sourceforge.net/index.shtml) [19], which was set up to report only uniquely aligning reads. Duplicate reads were removed using Samtools (version 0.1.18) [20]. The ChIP analysis was performed using the Homer (version 3.9) suite of tools (biowhat.ucsd.edu/homer/ngs/index.html) [21]. The pipeline for the analysis is shown in Supplementary Fig. 1. Custom scripts were created to compare the list of known genes closest to ChIP peaks with gene lists generated from RNA microarray experiments. These corroborated gene lists were visualised on chromosomes using Circos plots (circos.ca; Supplementary Fig. 2) and Venn diagram (Fig. 2b).



2.8. Reverse transcription PCR (RT-PCR)

Total RNA isolation was extracted from MEF WT and MEF –/– cells using an RNeasy Mini Kit (Qiagen) according to the manufacturer's instructions. RT-PCR reactions were carried out using the OneStep RT-PCR Kit from Qiagen. Briefly, 5–10 ng of RNA per sample was used in 25 μ l reaction mixture containing 0.4 mM

a
Validation of C/EBPβ ChIP-Sequencing

| Rank | Motif | P-value | log P-value | % of Targets | % of Background | STD(Bg STD) | Best Match/Details |
|------|---|---------|-------------|--------------|-----------------|-----------------|---------------------------------------|
| 1 |  | 1e-128 | -2.955e+02 | 15.12% | 3.09% | 47.1bp (58.8bp) | CEBP(bZIP)/CEBPb-ChIP-Seq/Homer |
| 2 |  | 1e-69 | -1.604e+02 | 9.61% | 2.26% | 52.6bp (59.4bp) | CEBP:AP1/ThioMac-CEBPb-ChIP-Seq/Homer |

Validation of C/EBPδ ChIP-Sequencing

| Rank | Motif | P-value | log P-value | % of Targets | % of Background | STD(Bg STD) | Best Match/Details |
|------|---|---------|-------------|--------------|-----------------|-----------------|---------------------------------------|
| 1 |  | 1e-869 | -2.002e+03 | 58.50% | 6.49% | 39.9bp (61.4bp) | MA0102.2_CEBPA |
| 2 |  | 1e-49 | -1.134e+02 | 6.22% | 1.23% | 57.1bp (62.1bp) | CEBP:AP1/ThioMac-CEBPb-ChIP-Seq/Homer |

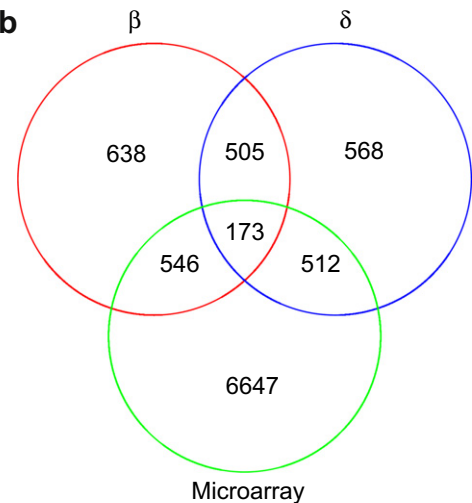


Fig. 2. Results of C/EBPβ and C/EBPδ ChIP-SEQ and microarray. a) MEF WT cells were incubated in the presence or absence of a combination of the cyclic AMP-elevating agents, forskolin and rolipram (F/R). Following stimulation cells were fixed, chromatin was isolated and then immunoprecipitated (ChIP'd) with anti-C/EBPβ or C/EBPδ antibodies, as described in Materials and methods. ChIP'd DNA samples were then sequenced (ChIP-SEQ) on an Illumina GA IIx DNA sequencer. ChIP analysis of the resulting DNA sequences was then performed using the Homer (version 3.9) suite of tools (biowhat.ucsd.edu/homer/ngs/index.html). The figure shows part of the Homer analysis indicating that aligned sequences from each ChIP experiments contained *bona fide* C/EBP consensus binding motifs, hence validating the experimental technique. b) MEF WT, MEF C/EBPβ ^{-/-} and MEF C/EBPδ ^{-/-} cells were stimulated for 5 h in the presence or absence of F/R. Cells were then harvested, RNA isolated, biotinylated sense-strand DNA synthesised and hybridised to mouse whole genome GeneChip® ST Arrays (Affymatrix). A Venn diagram was then generated to illustrate the degree of overlap between genes identified by ChIP-SEQ as containing consensus, F/R-dependent C/EBP-binding sites and F/R-induced changes in MEF gene expression.

dNTPs and 0.6 μM of each primer. The primer sequences used were mTubb2a (Fwd 5'-TGTGTACTACAATGAAGCTG, Rev 5'-GGTACTCCTCTCTGATCTTG), mRnd3 (Fwd 5'-ATATGGCCAAGCAGATCGGA, Rev 5'-TCACAGTACAGCTCTTCGCT), mKrt16 (Fwd 5'-GGAAATGCAGATTGAAAACC, Rev 5'-CATACAGTATCTGCCTTTGG), mKrt20 (Fwd 5'-ACTACGCACAGATTAAGAG, Rev 5'-TCCAAGTCTGTCTTTGAAG), mNR4a3 (Fwd 5'-ATGAACCCCGACTACACCAA, Rev 5'-GTAGAAGGCGGAGACTGCTT), mIRS (Fwd 5'-ACTATATGCCCATGAGCCCC, Rev 5'-AGTAAGAGAGGACCGGCTTG), mIL6 (Fwd 5'-AAATGATGGATGCTACCAAA, Rev 5'-TGACTCCAGCTTATCTGTTA) and mActin (Fwd 5'-GGTCATCACTATTGGCAACG, Rev 5'-ACGGATGTCAACGTCACACT). Reactions were carried out in a thermocycler with the following settings; 30 min at 50°C (RT-PCR), 15 min at 95°C (hot-start) and then 30 cycles of 30 s at 94°C, 30 s at 50°C followed by 1 min at 72°C followed by 10 min at 72°C. PCR products were visualised following ethidium bromide staining on agarose gels.

3. Results and discussion

3.1. The role of C/EBPδ in controlling cell adhesion and spreading on nanometric grooves

In order to determine the role of C/EBPδ transcription factor in regulating cell interaction with nanometric topology, embryonal fibroblasts isolated from wild type (MEF WT), or transgenic mice in which both alleles encoding C/EBPδ had been deleted (MEF C/EBPδ ^{-/-}), were grown on planar or nanogroove (240 nm or 540 nm depth, fixed 12.5 μm groove/ridge width (25 μm pitch)) surfaces.

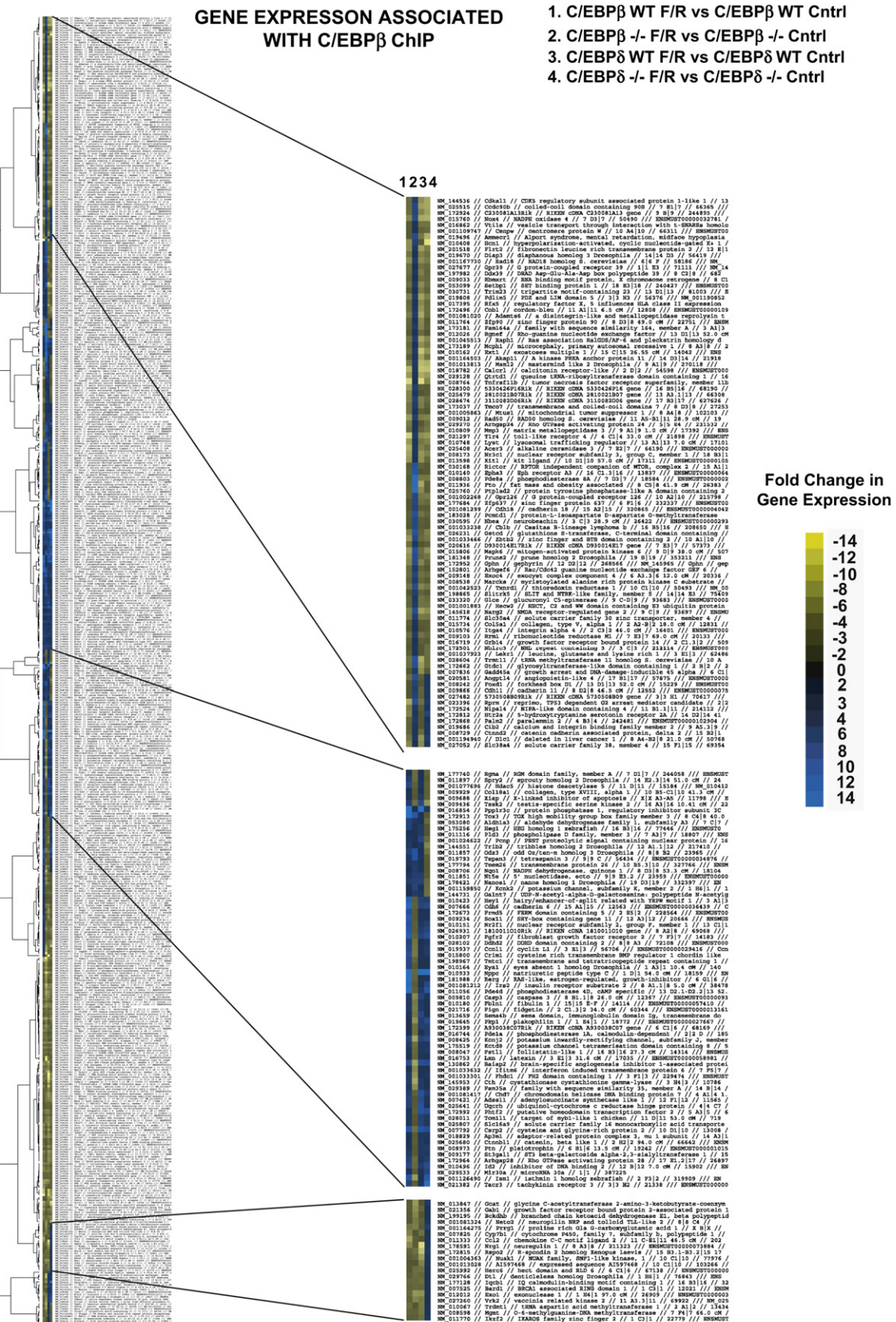
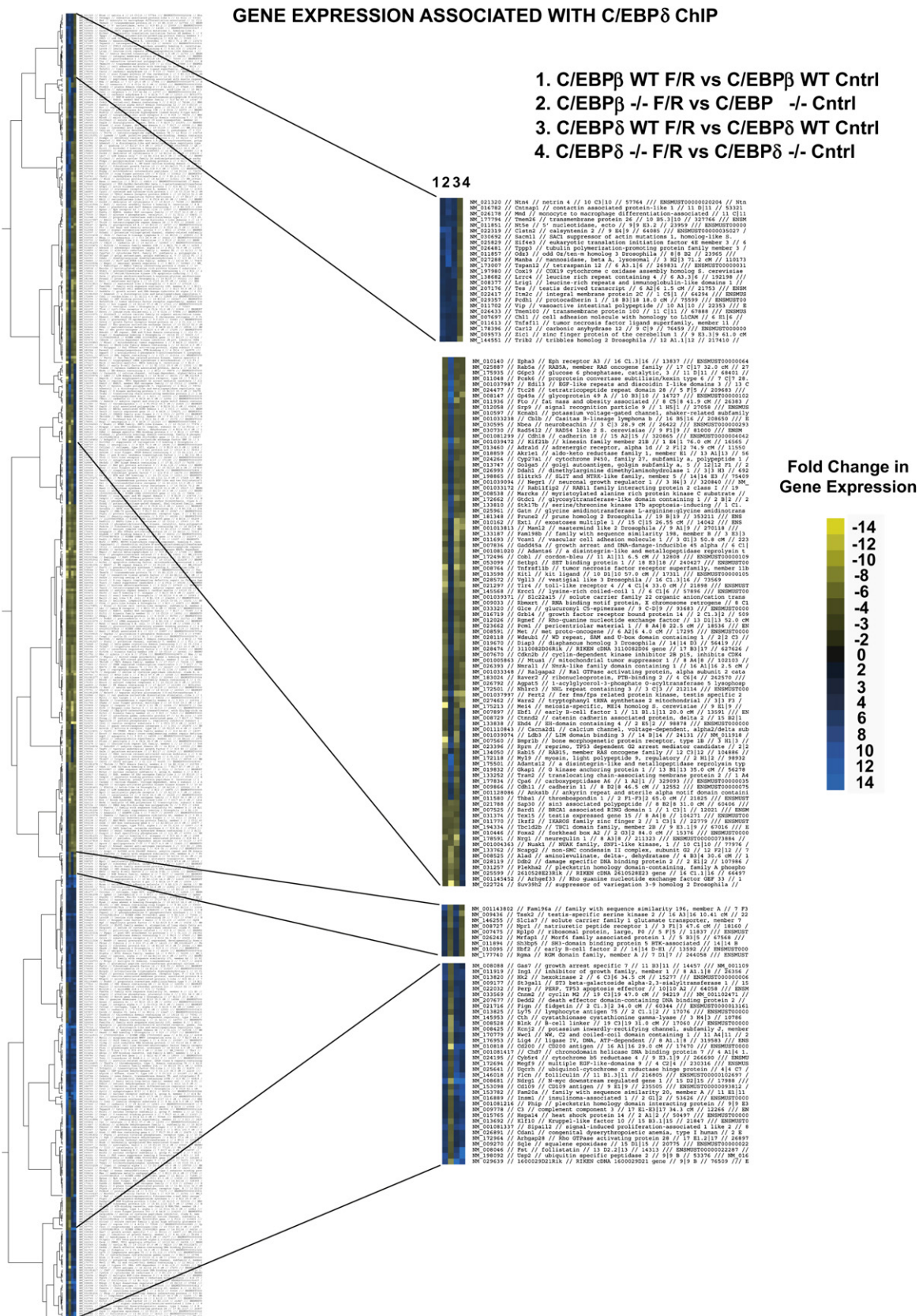


Fig. 3. Gene expression changes from microarray that are also identified by C/EBP β ChIP-SEQ microarray analysis was carried out on RNA samples isolated from MEF WT, MEF C/EBP β $-/-$ and MEF C/EBP δ $-/-$ cells that had been stimulated in the presence or absence (CNTRL) of F/R for 5 h. Gene expression ratios from all cell types were then matched with genes identified from ChIP-SEQ as containing C/EBP β binding sites. CLUSTER analysis was then used to generate a dendrogram (on the left) to group together gene changes with similar expression profiles. The enlarged sections on the right represent groups of genes that are either induced (blue) or repressed (yellow) following F/R treatment and display a dependency for either C/EBP β , C/EBP δ or both, as represented by a directional change in gene expression in samples isolated from either MEF C/EBP β $-/-$ or MEF C/EBP δ $-/-$ cells. (For interpretation of the references to colour in this figure legend, the reader is referred to the web version of this article.)



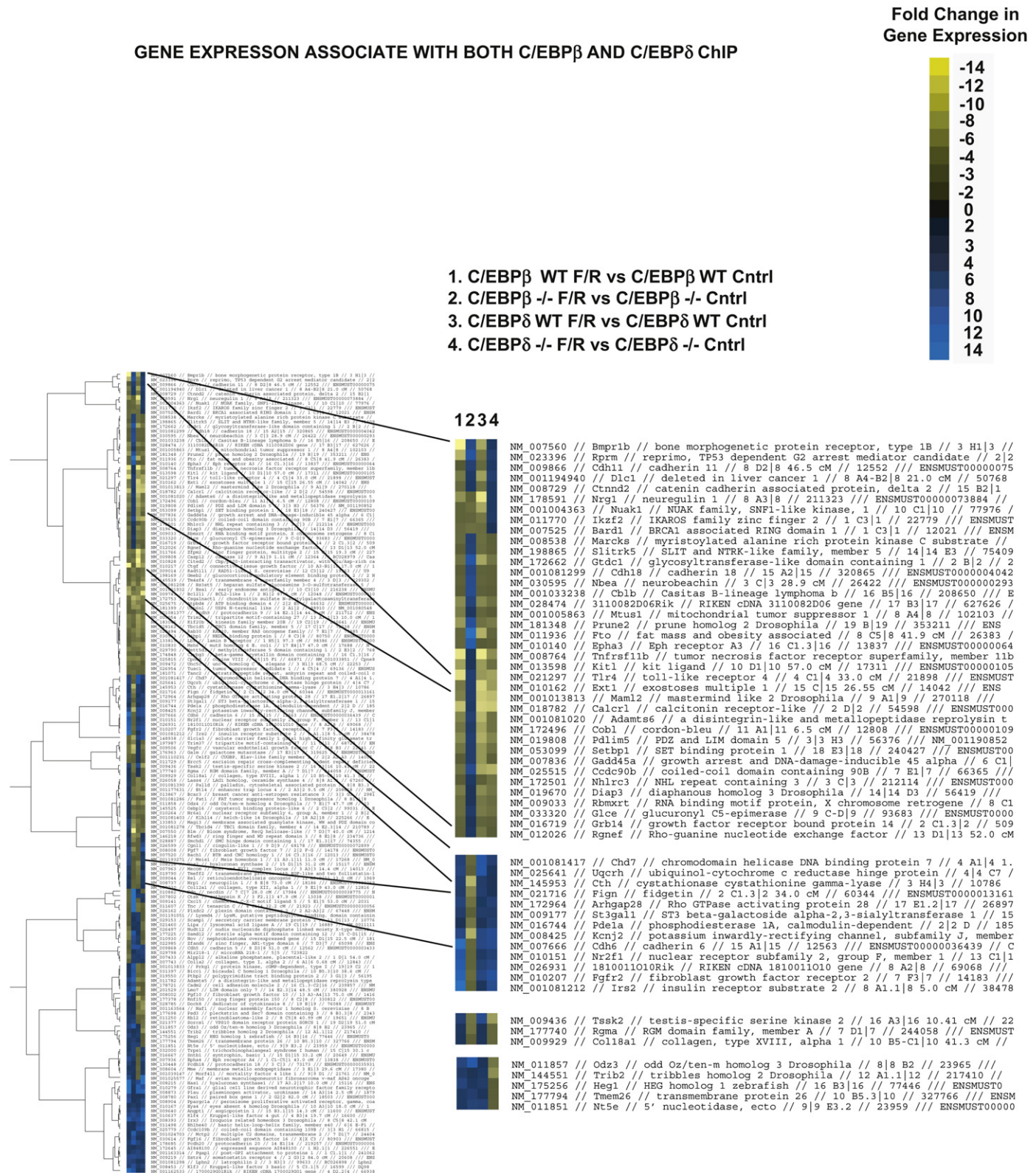


Fig. 5. Gene expression changes from microarray that are also identified by both C/EBP β and C/EBP δ ChIP-SEQ CLUSTER analysis was carried out on microarray gene expression changes that were also identified by ChIP-SEQ as genes with consensus binding sites for both C/EBP β and C/EBP δ ChIP.

Cells were then fixed and immunostained with anti-actin and anti-vinculin antibodies (Fig. 1a). From these experiments it was apparent that MEF WT cells spread normally on planar growth surfaces, possessing a well developed actin cytoskeleton and

adhesion complexes, as indicated by phalloidin and vinculin staining respectively. In addition, MEF WT cells grown on 240 nm or 540 nm grooves became more elongated and aligned themselves along the direction of the nanogrooves (Fig. 1a). In contrast, MEF C/

GENE EXPRESSION ASSOCIATED WITH NEITHER C/EBP β OR C/EBP δ ChIP

Fold Change in
Gene Expression



- 1.C/EBP β WT F/R vs C/EBP β WT Cntrl
- 2.C/EBP β -/- F/R vs C/EBP β -/- Cntrl
- 3.C/EBP δ WT F/R vs C/EBP δ WT Cntrl
- 4.C/EBP δ -/- F/R vs C/EBP δ -/- Cntrl

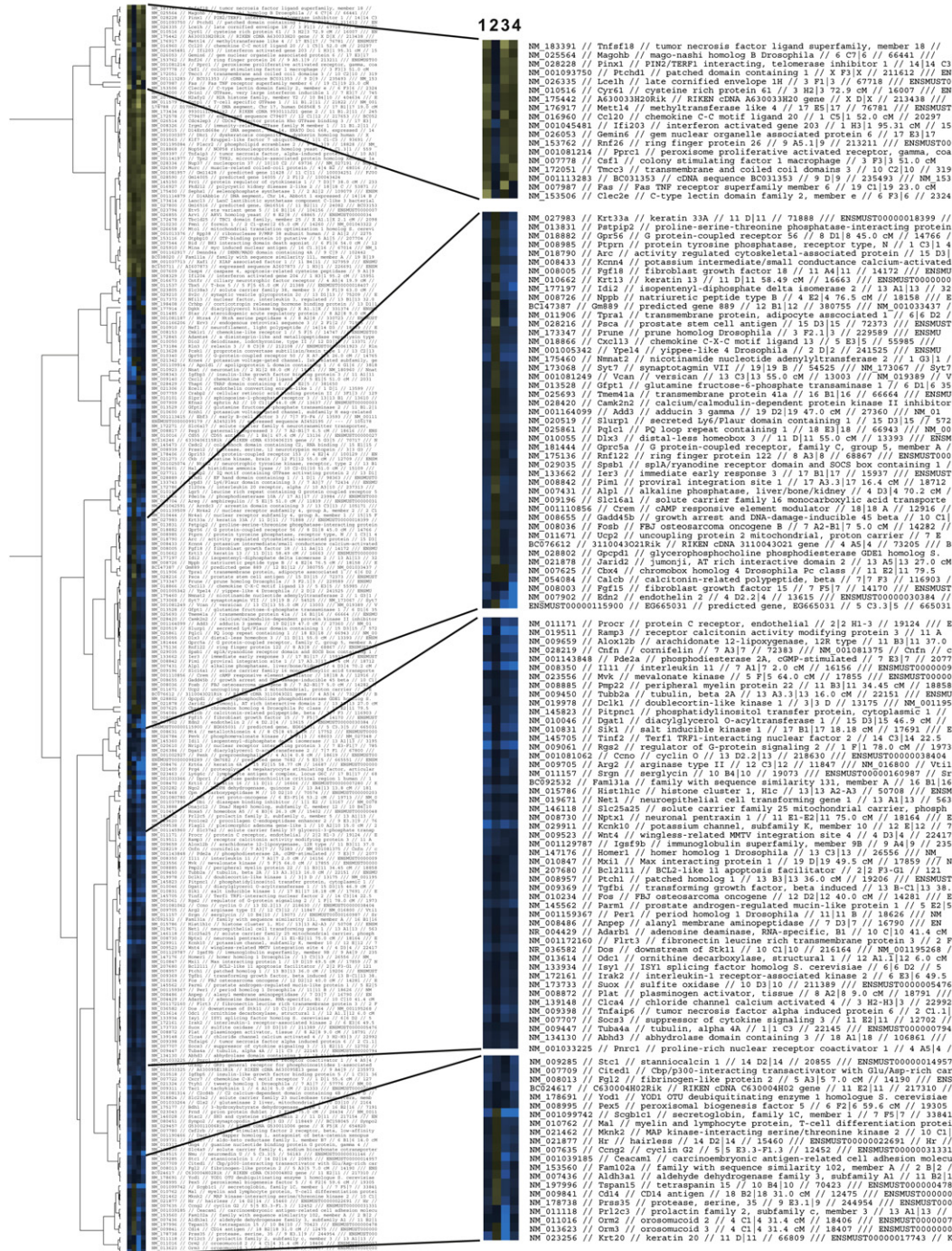


Fig. 6. Gene expression changes from microarray that were not identified by either C/EBP β or C/EBP δ ChIP-SEQ. CLUSTER analysis was carried out on microarray gene expression changes on genes that were not identified by either C/EBP β or C/EBP δ ChIP-SEQ. These gene identities probably represent genes that are either regulated by F/R, independently of C/EBP β or C/EBP δ , or genes that are trans-activated by C/EBP β or C/EBP δ .

EBP δ $-/-$ cells grown on a flat substrate were more rounded, with a poorly developed actin cytoskeleton and reduced focal adhesions, as demonstrated by a reduction in vinculin staining (Fig. 1b). MEF C/EBP δ $-/-$ cells also appeared more stellate with extensive arborisation and, although they underwent contact guidance on nanometric grooves, became much more elongated and were much less spread than MEF WT cells, particularly on 540 nm grooves. These results demonstrate that the transcription factor C/EBP δ plays an essential role in efficient adhesion and spreading to both planar and nanometric grooved surfaces. These results are consistent with a recent report demonstrating that MEF C/EBP δ $-/-$ cells display increased migration when compared with MEF WT cells in wound healing assays [22] and suggests that C/EBP δ may play a role in regulating the expression of genes involved in cell adhesion, movement and spreading.

3.2. Identification of C/EBP δ consensus binding sites within the mouse genome

In order to test whether C/EBP δ does in fact regulate gene expression associated with interactions with cell growth surfaces we carried out genomic analysis to identify the full range of genes and gene promoters regulated by C/EBP δ in MEFs. We stimulated MEF WT and MEF C/EBP δ $-/-$ cells for 5 h with a combination of the pharmacological agents (F/R), forskolin, which promotes cyclic AMP

synthesis, and rolipram, which inhibits cyclic AMP degradation, to increase the intracellular levels of C/EBP δ protein through the activation of the C/EBP δ gene [17] (Fig. 8). As a comparison, and to ensure that we could identify genes specifically regulated by C/EBP δ , C/EBP β WT and $-/-$ cells were treated in a similar fashion. This was done because many of the cellular actions of C/EBP δ are shared by C/EBP β [17]. Following stimulation MEF WT cells were fixed, lysed and cellular chromatin isolated, fragmented and immunoprecipitated (ChIP) with anti-C/EBP δ or anti-C/EBP β antibodies. The genomic DNA associated with ChIP'd samples was then sequenced using a genome analyser (ChIP-SEQ) to identify the C/EBP δ are C/EBP β binding sites throughout the genome. The sequence reads were aligned to the mouse genome using the Bowtie aligner (version 0.12.7), which was set up to report only uniquely aligning reads, and duplicate reads were removed using Samtools (version 0.1.18). The Homer (version 3.9) suite of tools was used to verify that the majority of reads contained bone fide C/EBP-binding sites (Fig. 2a).

To complement the ChIP-SEQ analysis, mRNA was also extracted from F/R-treated MEF C/EBP δ WT, MEF C/EBP δ $-/-$, MEF C/EBP β WT and MEF C/EBP β $-/-$ cells. The extracted mRNA was then converted by reverse transcription to cDNA probes, which were then hybridised to mouse whole genome microarrays (Affymetrix). This approach was used so as to determine whether the genes that contain C/EBP-binding sites, identified by ChIP-SEQ, are also regulated at the level of transcription in a C/EBP-dependent manner.

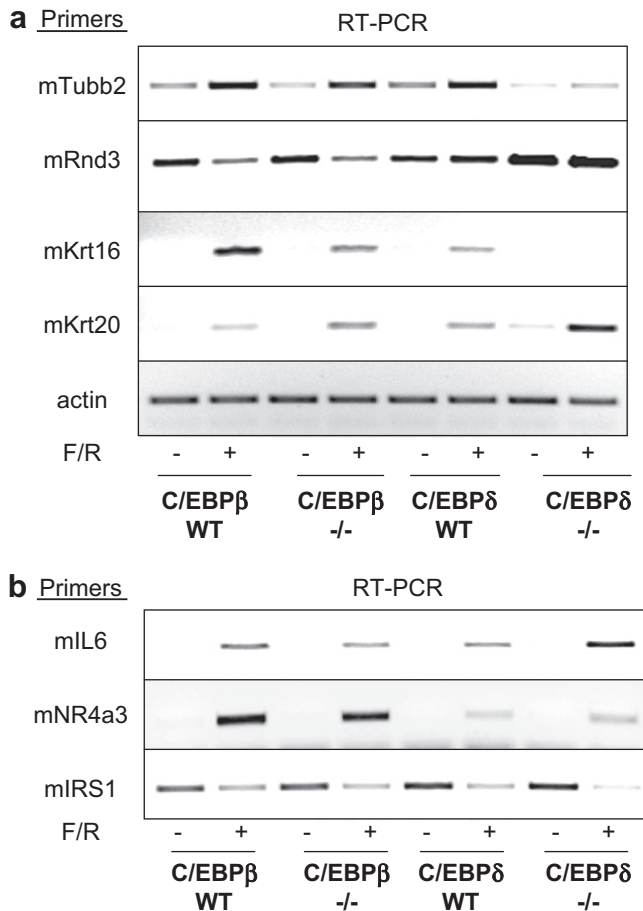


Fig. 7. RT-PCR analysis demonstrates that C/EBP δ is required for the regulation of genes encoding cytoskeletal components and IL6. MEF WT or MEF $-/-$ cells were incubated for 5 h with a combination of forskolin and rolipram (F/R), following which RNA was extracted, reverse transcribed and PCR amplified using the indicated primers. Results demonstrate that F/R regulates the expression of mRNAs encoding cytoskeletal components (a) and IL6 (b) in a C/EBP δ -dependent manner.

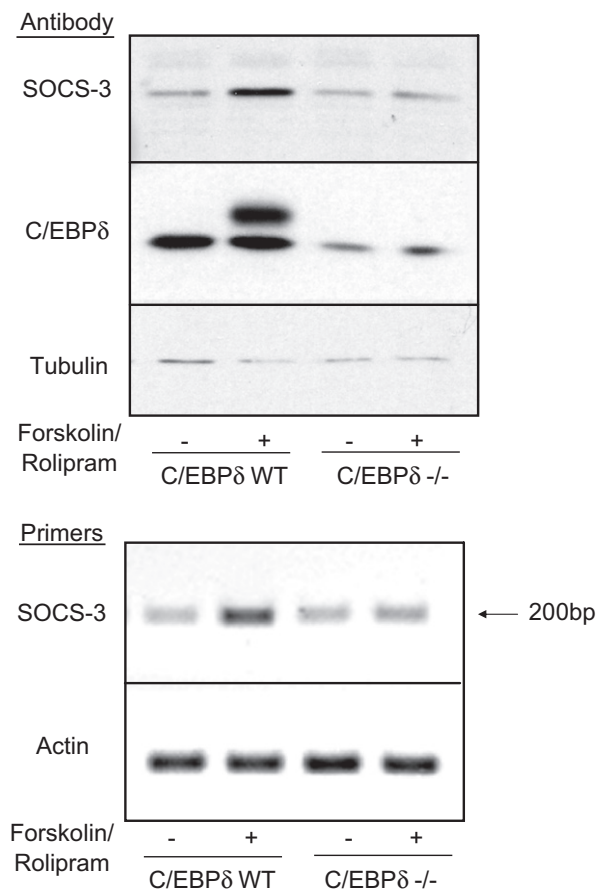


Fig. 8. Deletion of the C/EBP δ gene in MEFs blocks the induction of SOCS3 mRNA and protein. MEF WT and MEF C/EBP δ $-/-$ cells were stimulated for 5 h with F/R to elevate intracellular cyclic AMP levels. This resulted in the induction of C/EBP δ and SOCS3 protein in MEF WT, but not MEF C/EBP δ $-/-$, cells as detected by Western blotting in the upper panel. Deletion of the C/EBP δ gene also blocked the ability of F/R to induce SOCS3 mRNA expression, as detected by RT-PCR (lower panel).

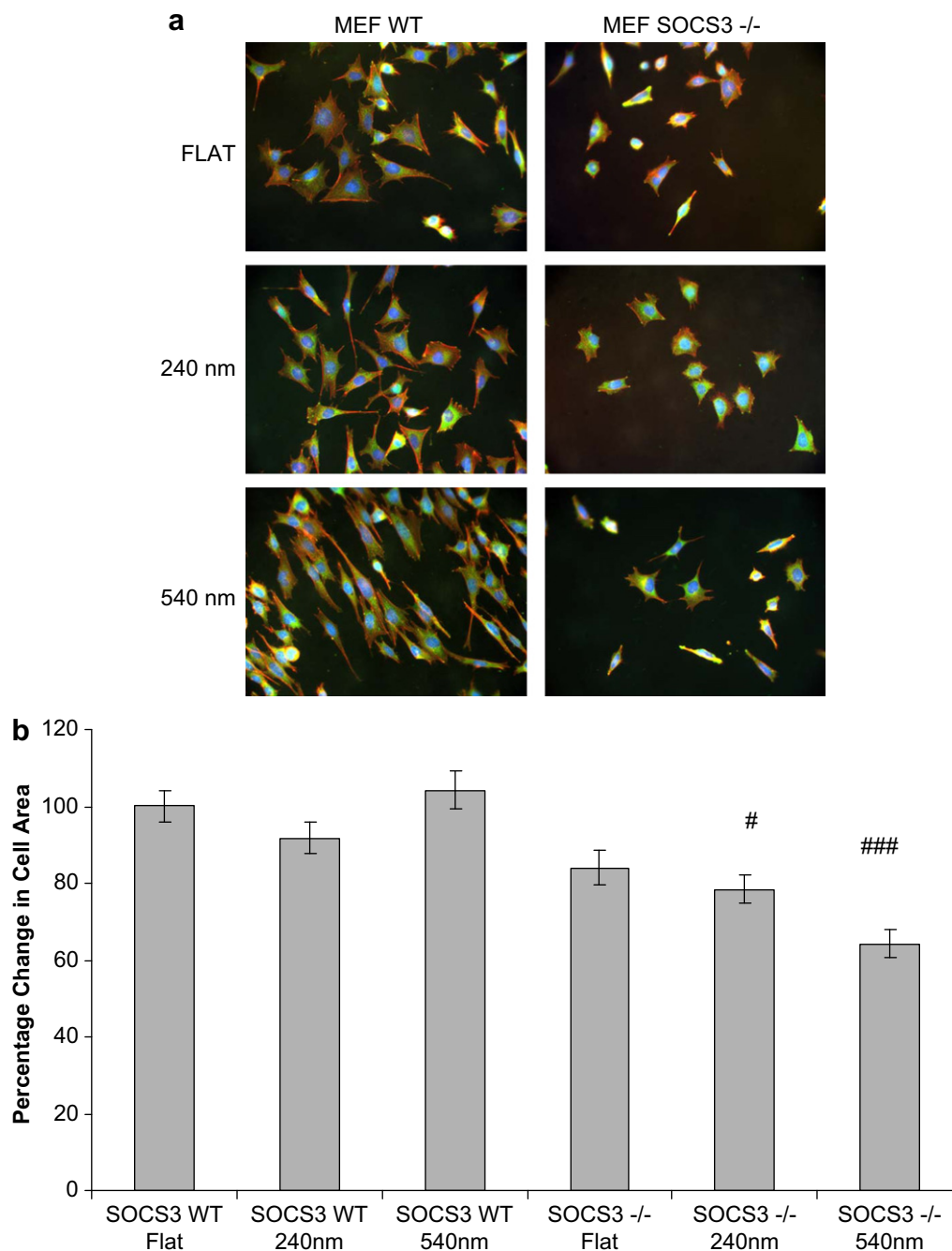


Fig. 9. Morphology of Wild Type (WT) and SOCS3 $-/-$ MEFs Cultured on Flat or Nanogrooved Substrates MEF WT and MEF SOCS3 $-/-$ cells were cultured on flat or nanogrooved substrates and stained for actin cytoskeleton (red) and vinculin (green). It can be seen in (a) that C/EBP $-/-$ MEFs were smaller and had a poorly developed actin cytoskeleton and were unable to contact align to nanogrooved substrates. MEF WT and MEF SOCS3 $-/-$ cell area (b) and vinculin intensity (c) were quantified as described in Materials and Methods. Results demonstrated that MEF SOCS3 $-/-$ cells were smaller and had lower levels of vinculin (c) on nanogrooved surfaces, than MEF WT cells. Western blotting with anti-SOCS3 antibodies (d) demonstrated that MEF WT cells also expressed significantly lower levels of SOCS3 protein on 540 nm nanometric grooves. (For interpretation of the references to colour in this figure legend, the reader is referred to the web version of this article.)

Genes identified as being regulated by F/R, or by deletion of either C/EBP δ or C/EBP β , are listed in [Supplementary Data Set 2](#). Custom scripts were then created to compare the list of known genes closest to ChIP peaks with gene lists generated from RNA microarray experiments ([Supplementary Data Set 1](#)).

These corroborated gene lists were visualised on chromosomes using Circos plots (circos.ca; [Supplementary Fig. 2](#)) and a Venn diagram ([Fig. 2b](#)). From these analyses we identified over 1100 genes that interact with C/EBP β alone and a similar number that

interact with C/EBP δ alone ([Fig. 2b](#); [Supplementary Data Set 1](#)). Over 650 genes contain binding sites for both C/EBP β and C/EBP δ ([Fig. 2b](#); [Supplementary Data Set 1](#)). Generally, C/EBP β and C/EBP δ binding sites were distributed evenly throughout the cellular chromosomes ([Supplementary Fig. 2](#)). Of the approximate 7800 genes identified by cDNA microarray as being regulated by the F/R treatment regime ([Supplementary Data Set 2](#)), over 500 were identified as containing C/EBP β binding sites, over 500 contained C/EBP δ binding sites and over 170 contained binding sites for both C/EBP β and C/EBP δ .

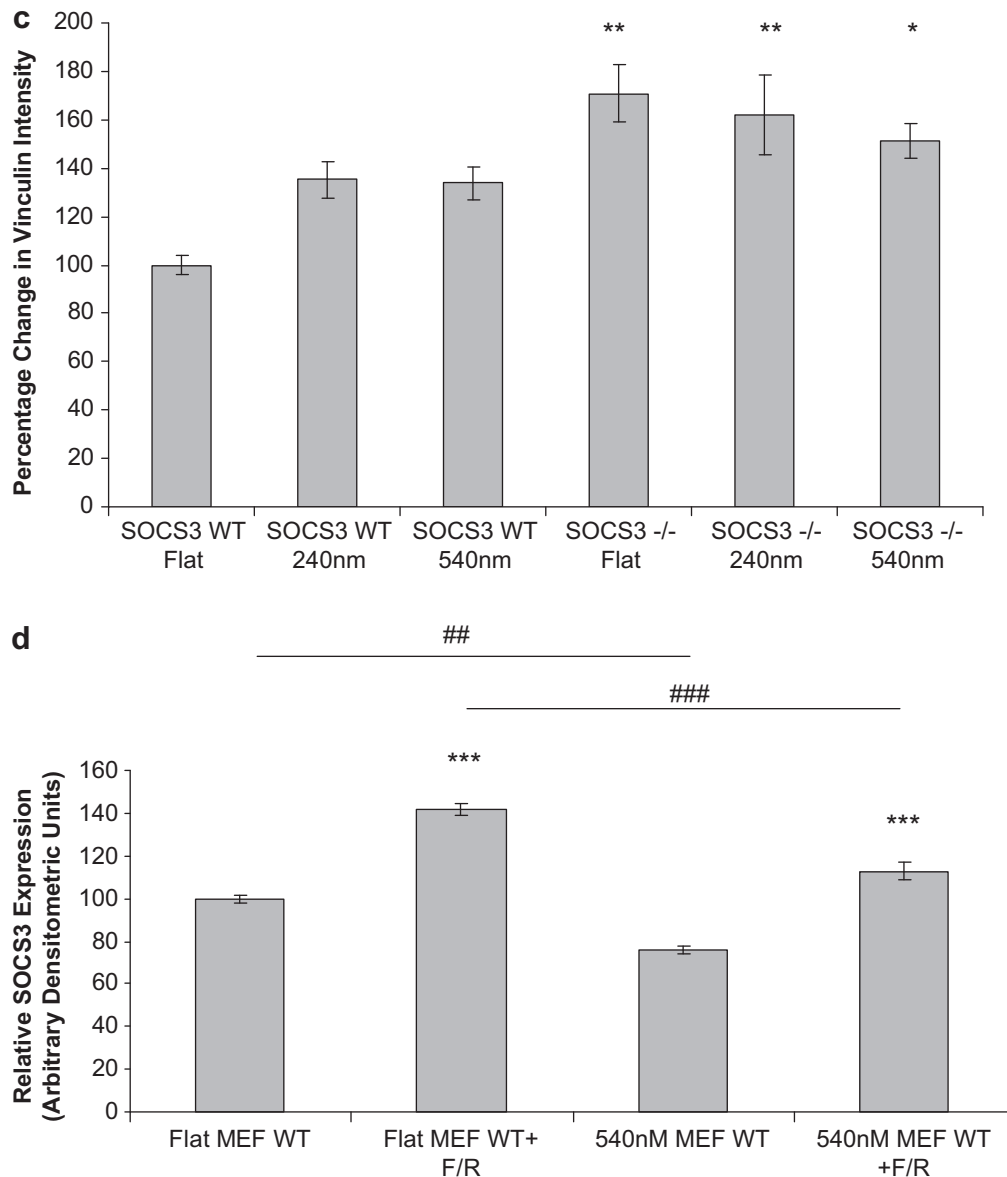


Fig. 9. (continued).

(Fig. 2b; Supplementary Data Set 1). These figures far exceed the approximate 100 C/EBP δ target genes previously identified through ChIP–chip assays in a previous study [8] and demonstrates the sensitivity of our combined ChIP–SEQ and cDNA microarray approach. Taken together our data demonstrates that C/EBP β and C/EBP δ isoforms interact promiscuously with the mouse genome through direct interaction multiple C/EBP-binding sites. Moreover, the fact that C/EBP δ specifically interacts with over 1000 genes, independently of C/EBP β , suggests that C/EBP δ may play a unique and specific role in the control of cell behaviour through the independent regulation of multiple gene regulatory networks.

3.3. Identification of genes whose expression is specifically regulated by C/EBP δ

Results this far indicate that there are many regulatory C/EBP δ binding sites distributed throughout the mouse genome. Accordingly, the identities of genes that contain C/EBP δ binding sites are diverse and don't immediately describe shared functions (Supplementary Data Set 1). The same can be said for C/EBP β -interacting genes

(Supplementary Data Set 1). Therefore, in order to further delineate the function of C/EBP δ in MEFs we carried out CLUSTER analysis [18] on the F/R-induced gene expression changes that were identified by both cDNA microarray and SEQ analysis (Supplementary Data Set 2). CLUSTERS were generated for gene expression changes associated with C/EBP β (Fig. 3), C/EBP δ (Fig. 4) and shared (C/EBP β plus C/EBP δ ; Fig. 5) ChIP–SEQ and therefore represent genes that are potentially cis-regulated by C/EBPs β and/or δ . From these results in can be seen that F/R stimulation effects the induction or suppression of a large number of genes, where the direction of change is similar between MEF WT and MEF $-/-$ cells (Figs. 3–5). This indicates that although C/EBPs β and/or δ physically interact with these genes, they do not appear to be required for transcriptional regulation by F/R. In contrast, CLUSTER analysis did reveal a number of gene groups (the enlarged portions of Figs. 3–5) that share a common expression patterns characterised by a directional change in gene expression relative to MEF WT cells, in one or both of MEF C/EBP β $-/-$ and/or MEF C/EBP δ $-/-$ cells, indicating a dependency on C/EBP β and/or C/EBP δ for the expression change. However, examining the majority of gene identities from C/EBP δ -dependent CLUSTERS, it is not immediately clear

which genes might be directly responsible for the effects of C/EBP δ on cell adhesion, migration and spreading that we observed on planar and nanometric growth surfaces (Fig. 1). We did note, however, that the RHO guanine nucleotide exchange factor 33 (ARHGEF33) appeared to be up-regulated in F/R-stimulated C/EBP δ $-/-$ cells (Fig. 4), indicating a possible link between C/EBP δ and the regulation of the tubulin cytoskeleton.

Surprisingly we could not find any other C/EBP δ -regulated, cytoskeleton linked gene identity in either of the C/EBP β or δ ChIP-SEQ lists, apart from RHO-family GTPase 3 (RND3), which was associated with C/EBP β ChIP, and hence is likely to be trans-, rather than cis-, activated by C/EBP δ . Consistent with a trans-activation role for C/EBP δ , we did find a number of genes encoding cytoskeleton components in Fig. 6 (tubulin β 2 (TUBB2), Keratin 16 (KRT16) and Keratin 20 (KRT20)), which details a CLUSTER of gene expression changes that do not match with ChIP-SEQ and therefore represent genes that are possibly trans-regulated by C/EBPs β and/or δ . Trans-regulation by C/EBP δ could occur through either the induction of expression of additional, “tertiary”, transcription factor(s) or through the activation of autocrine/paracrine signalling mechanisms. Interestingly, in this respect, F/R treatment was found to up-regulate the expression of the gene encoding the autocrine/paracrine cytokine interleukin 6 (IL6), which is a C/EBP δ -interacting gene whose expression was further enhanced in MEF C/EBP δ $-/-$ cells (Fig. 4). We confirmed this observation by RT-PCR analysis of IL6 mRNA levels in C/EBP WT and C/EBP $-/-$ cells (Fig. 7b) and contrasted these effects with the expression levels of the transcription factor nuclear receptor (NR) 4a3 and the signal transduction intermediate, insulin receptor substrate (IRS) 1, whose mRNA levels were either induced or repressed, respectively, following F/R treatment, but were unaffected by knockout of the C/EBP δ gene (Fig. 7b). Moreover, RT-PCR analysis confirmed that the genes encoding TUBB2, RND3, KRT16 and KRT20 were also induced by F/R treatment, consistent with a potential intermediary role for IL6, however only Krt20 was the only cytoskeletal component to be further induced following C/EBP δ deletion, whereas TUBB2 and KRT16 expression was suppressed (Fig. 7a). Basal levels of RND3 levels were enhanced in MEF C/EBP $-/-$ cells, whereas actin levels were unchanged, demonstrating that C/EBP δ is a general repressor of RND3 gene activity (Fig. 7a).

Together these results demonstrate that C/EBP δ plays a central role in the regulated expression of cytoskeleton components (TUBB2, KRT16 and KRT20) and cytoskeleton regulators (ARHGEF33 and RND3) in MEFs. Since no direct interaction was detected between C/EBP δ and the genes encoding these cytoskeletal components, it is likely that an intermediary, trans-activating element, such as C/EBP δ -regulated IL-6 (Fig. 7b), may be required for their regulation. These observations may go some way to explain the requirement for C/EBP δ for proper adhesion and spreading on planar and nanometric growth surfaces described in Fig. 1.

3.4. The role of SOCS3 in spreading and contact guidance on nanometric grooves

Another potential target for IL6-mediated, C/EBP δ -dependent trans-activation is the suppressor of cytokine signalling 3 (SOCS3) gene. SOCS3 is known to be a direct target of IL6-receptor activation, mediated by tyrosine phosphorylated STAT3 transcription factors [23]. Moreover, we have shown that SOCS3 gene induction is absolutely required for efficient SOCS3 induction by F/R in vascular endothelial cells [17]. In the present study, we identified SOCS3 as being induced by C/EBP δ -dependent F/R treatment of MEFs in microarray experiments (Fig. 6), Western blotting (Fig. 8a) and RT-PCR (Fig. 8b), but not in ChIP-SEQ analysis. The SOCS3 gene encodes an E3 ubiquitin ligase which targets focal adhesion-associated FAK tyrosine kinase for proteolytic degradation [24,25]

compared the abilities of MEF WT and MEF SOCS3 $-/-$ cell to attach and contact align to flat, 240 nm and 540 nm grooved growth surfaces (Fig. 9). We found that, as with previous experiments, MEF WT cells attached and aligned to nanometric grooves effectively (Fig. 9a). In contrast, MEF SOCS3 cells had an altered morphology, characterised by enhanced vinculin expression, and failed to contact align to either 240 nm or 540 nm grooves (Fig. 9a and b). Consistent with a role for SOCS3 in controlling contact guidance, SOCS3 protein levels were found to be significantly reduced in MEF WT cells (Fig. 9c). In contrast to MEF SOCS3 $-/-$ cells, MEF FAK $-/-$ cells did not show any appreciable difference in their ability to adhere and contact align to nanometric grooves (Supplementary Fig. 3a and b). This indicates that the requirement of SOCS3 for efficient alignment to nanometric grooves is independent of its ability to regulate FAK protein levels in cells.

4. Conclusions

In summary, we have used genomic analysis to demonstrate that C/EBP δ is a transcription factor that is required for efficient attachment, spreading and alignment to nanometric grooves. This appears to occur through the trans-activation of genes encoding inducible cell signalling elements, such as SOCS3, cytoskeletal components, such as TUBB2, KRT16 and KRT20, and cytoskeletal regulators, such as ARHGEF33 and RND3. A possible mechanism for this trans-activation is through the cis-regulated induction of autocrine/paracrine mediators, such as IL6. Of these newly identified, C/EBP δ -regulated genes, SOCS3 was found to be absolutely required for cells to be able to attach, align and spread on nanometric grooves. The fact that the effects of C/EBP δ knockout on the interaction with nanometric grooves are much more subtle than those observed with SOCS3 knockout, suggests that the effects brought about by the loss of cellular C/EBP δ can, to some extent, be compensated for by cellular C/EBP β , which we find to interact and regulate many of the same genes as C/EBP δ (Fig. 2b). Overall this study demonstrates the complexity of C/EBP δ -controlled gene regulation and its importance for determining the nature of cell interactions with extracellular, nanometric cues.

Acknowledgements

This work was supported by the British Heart Foundation [Grants PG/10/026/28303 and PG/08/125/26415] awarded to SJY.

Appendix A. Supplementary data

Supplementary data related to this article can be found at <http://dx.doi.org/10.1016/j.biomaterials.2012.11.036>.

References

- [1] Ramji DP, Foka P. CCAAT/enhancer-binding proteins: structure, function and regulation. *Biochem J* 2002;365(Pt 3):561–75.
- [2] Barbaro V, Testa A, Di Iorio E, Mavilio F, Pellegrini G, De Luca M. c/ebp delta regulates cell cycle and self-renewal of human limbal stem cells. *J Cell Biol* 2007;177(6):1037–49.
- [3] O'Rourke J, Yuan R, DeWille J. CCAAT/enhancer-binding protein-delta (c/ebp-delta) is induced in growth-arrested mouse mammary epithelial cells. *J Biol Chem* 1997;272(10):6291–6.
- [4] Porter DA, Krop IE, Nasser S, Sgroi D, Kaelin CM, Marks JR, et al. A SAGE (serial analysis of gene expression) view of breast tumor progression. *Cancer Res* 2001;61(15):5697–702.
- [5] Tang D, DeWille J. Detection of base sequence changes in the cebpd gene in human breast cancer cell lines and primary breast cancer isolates. *Mol Cell Probes* 2003;17(1):11–4.
- [6] Porter D, Lahti-Domenici J, Keshaviah A, Bae YK, Argani P, Marks J, et al. Molecular markers in ductal carcinoma in situ of the breast. *Mol Cancer Res* 2003;1(5):362–75.

- [7] Agrawal S, Hofmann WK, Tidow N, Ehrich M, van den Boom D, Koschmieder S, et al. The *c/ebp delta* tumor suppressor is silenced by hypermethylation in acute myeloid leukemia. *Blood* 2007;109(9):3895–905.
- [8] Zhang Y, Liu T, Yan P, Huang T, Dewille J. Identification and characterization of CCAAT/enhancer binding protein delta (*c/ebp delta*) target genes in G0 growth arrested mammary epithelial cells. *BMC Mol Biol* 2008;9:83.
- [9] Gigliotti AP, Johnson PF, Sterneck E, DeWille JW. Nulliparous CCAAT/enhancer binding protein delta (*c/ebp delta*) knockout mice exhibit mammary gland ductal hyperplasia. *Exp Biol Med* (Maywood) 2003;228(3):278–85.
- [10] Cao Z, Umek RM, McKnight SL. Regulated expression of three *c/ebp* isoforms during adipose conversion of 3T3-L1 cells. *Genes Dev* 1991;5(9):1538–52.
- [11] Farmer SR. Transcriptional control of adipocyte formation. *Cell Metab* 2006;4(4):263–73.
- [12] Zhang Y, Sif S, DeWille J. The mouse *c/ebp delta* gene promoter is regulated by stat3 and sp1 transcriptional activators, chromatin remodeling and c-myc repression. *J Cell Biochem* 2007;102(5):1256–70.
- [13] Hutt JA, O'Rourke JP, DeWille J. Signal transducer and activator of transcription 3 activates CCAAT enhancer-binding protein delta gene transcription in G0 growth-arrested mouse mammary epithelial cells and in involuting mouse mammary gland. *J Biol Chem* 2000;275(37):29123–31.
- [14] Li B, Si J, DeWille JW. Ultraviolet radiation (uvr) activates p38 map kinase and induces post-transcriptional stabilization of the *c/ebp delta* mRNA in G0 growth arrested mammary epithelial cells. *J Cell Biochem* 2008;103(5):1657–69.
- [15] Zhou S, Dewille JW. Proteasome-mediated CCAAT/enhancer-binding protein delta (C/EBPdelta) degradation is ubiquitin-independent. *Biochem J* 2007;405(2):341–9.
- [16] Zhou S, Si J, Liu T, DeWille JW. PIASy represses CCAAT/enhancer-binding protein delta (*c/ebp delta*) transcriptional activity by sequestering *c/ebp delta* to the nuclear periphery. *J Biol Chem* 2008;283(29):20137–48.
- [17] Yarwood SJ, Borland G, Sands WA, Palmer TM. Identification of CCAAT/enhancer-binding proteins as exchange protein activated by camp-activated transcription factors that mediate the induction of the *socs-3* gene. *J Biol Chem* 2008;283(11):6843–53.
- [18] Eisen MB, Spellman PT, Brown PO, Botstein D. Cluster analysis and display of genome-wide expression patterns. *Proc Natl Acad Sci U S A* 1998;95(25):14863–8.
- [19] Langmead B, Trapnell C, Pop M, Salzberg SL. Ultrafast and memory-efficient alignment of short DNA sequences to the human genome. *Genome Biol* 2009;10(3):R25.
- [20] Li H, Handsaker B, Wysoker A, Fennell T, Ruan J, Homer N, et al. The sequence alignment/map format and SAMtools. *Bioinformatics* 2009;25(16):2078–9.
- [21] Heinz S, Benner C, Spann N, Bertolino E, Lin YC, Laslo P, et al. Simple combinations of lineage-determining transcription factors prime cis-regulatory elements required for macrophage and B cell identities. *Mol Cell* 2010;38(4):576–89.
- [22] Yu X, Si J, Zhang Y, Dewille JW. CCAAT/enhancer binding protein-delta (*c/ebp-delta*) regulates cell growth, migration and differentiation. *Cancer* 2010;10:48.
- [23] Lesina M, Kurkowski MU, Ludes K, Rose-John S, Treiber M, Kloppel G, et al. Stat3/socs3 activation by IL-6 transsignaling promotes progression of pancreatic intraepithelial neoplasia and development of pancreatic cancer. *Cancer* 2011;19(4):456–69.
- [24] Liu E, Cote JF, Vuori K. Negative regulation of fak signaling by socs proteins. *Embo J* 2003;22(19):5036–46.
- [25] Niwa Y, Kanda H, Shikauchi Y, Saiura A, Matsubara K, Kitagawa T, et al. Methylation silencing of *socs-3* promotes cell growth and migration by enhancing jak/stat and fak signaling in human hepatocellular carcinoma. *Oncogene* 2005;24(42):6406–17.